OBSERVER BASED DYNAMIC SURFACE CONTROL OF A HYPERSONIC FLIGHT VEHICLE

W. A. Butt
Department of Electrical Engineering
College of Electrical and Mechanical Engineering
National University of Sciences and Technology, Pakistan
Email: butt_waseem@hotmail.com

Submitted: Feb. 12, 2013 ***Accepted: Mar. 19, 2013*** ***Published: Apr. 10, 2013***

Abstract- This paper describes the design and analysis of a proportional integral air speed controller and a nonlinear adaptive dynamic surface altitude controller for the longitudinal dynamics of a generic hypersonic flight vehicle. The uncertain nonlinear functions in the pure feedback flight vehicle model are approximated by using radial basis function neural networks. For the controller design, the complete states are assumed to be available for measurement, then a sliding mode observer is incorporated to estimate the states which are difficult to measure in practice. A detailed stability analysis of the designed altitude controller shows that all the signals of the closed loop system are uniformly ultimately bounded. The robustness and performance of the designed controllers, with and without the observer are verified through numerical simulations of the flight vehicle model for trimmed cruise conditions of 110,000 ft and Mach 15.

Index terms*:* Aircraft, adaptive control, dynamic surface control, neural networks, nonlinear systems, observer.

I. NOMENCLATURE

C_D	drag coefficient
C_L	lift coefficient
$C_M(q)$	pitching moment coefficient due to pitch rate
$C_M(\alpha)$	pitching moment coefficient due to angle of attack
$C_M(\delta_E)$	pitching moment coefficient due to elevator deflection
C_T	thrust coefficient
$\bar{c}$	reference length, ft
c_e	elevator coefficient
D	drag, lbf
h	altitude, ft
h_d	altitude demand, ft
I_{yy}	moment of inertia, slug-ft^2
k_h, k_q	observer sliding gains,1/s
k_α	observer sliding gain
k_γ	observer sliding gain, rad/ft.s
L	lift, lbf
M	Mach number
M_{yy}	pitching moment, lbf-ft
m	mass, slugs
q	pitch rate, rad/s
R_E	radius of earth, 20,903,500 ft
r	radial distance from Earth's center, ft
S	reference area, ft^2
S_1, S_2, S_3	surface errors
T	thrust, lbf
V	velocity, ft/s
V_d	desired velocity, ft/s
α	angle of attack, rad
$\alpha_1, \alpha_2, \alpha_3$	dynamic surface controller gains
β	throttle setting, % 100
δ_E	elevator deflection, rad
δ^*	network reconstruction error
η_{1ob}, η_{2ob}	observer damping coefficients, 1/s
η_{3ob}	observer damping coefficient, rad/ft.s
η_{4ob}	observer damping coefficient
$\eta_1, .., \eta_6$	update law gains
γ	flight-path angle, rad
γ_d	desired flight-path angle, rad
$\Gamma(.)$	update law diagonal gain matrix
θ_p	pitch angle, rad
τ_1, τ_2, τ_3	filter time constants
μ	gravitational constant, $1.39 \times 10^{16} ft^3/s^2$
ρ	density of air, slug/ft^3
σ	width of basis function
$\zeta_j \in R^N$	center of basis function

II. INTRODUCTION

Hypersonic flight vehicles may be the next generation means of cost effective and reliable transportation for both civil and military applications. The high speeds and endurance that these flight vehicles possess make them suitable candidates for prompt global responses, thus offering distinctive air superiority. The successful flight tests of the X-43A hypersonic test vehicle paved a way for further research and the application of the modern control design methodologies to such dynamic systems. A high fidelity mathematical model of the air-breathing hypersonic flight vehicle (AHFV) is usually not available, due to the difficulty in the precise measurement and estimation of the wind tunnel data. Also, due to the wide flight envelope, there is a marked

variation in the dynamic characteristics of the AHFVs, which introduces a high level of uncertainty. For safe and efficient flight of these types of vehicles, the onboard flight control system is required to deliver a superior performance and has to be robust to parametric uncertainties.

Flight control design of AHFVs poses a challenge due to the peculiar characteristic of the vehicle dynamics. In the last decade, considerable research efforts in the area of robust flight control design of AHFVs have resulted in the realization of actual flight tests. Robust control design techniques are well suited for design of flight controllers of AHFVs by virtue of their robustness to uncertainties. A number of linear robust controller design techniques exist that can be applied by using linearization of the nonlinear model at certain operating points. However, for ensuring stability at a wider range of operating points, the feedback linearization approach may be used to transform the nonlinear system into an equivalent linear system. Feedback linearization has been used with an adaptive sliding mode control to provide a robust solution [1], where the adaptive component is shown to circumvent the problem of control chattering. A robust solution is also obtained by using robust minimax Linear Quadratic Regulator design, which is based on a feedback linearized model of the nominal nonlinear dynamics of the AHFV with uncertain parameters [2]. Nonlinear dynamic inversion has also been utilized to assist in the design of robust controllers [3, 4]. For ensuring satisfactory performance of the aircraft for a wider flight envelope, the control structure requires an adaptive mechanism. Adaptive controller design methodology has found a place in the practical implementation after the successful test flight of such a controller in the USAF X-15 aircraft in 1959. An adaptive mechanism has been used in the backstepping and neural networks controller for the non linear flight dynamics system [5], but the backstepping control scheme suffers from the complexity of control law [6-9]. Recently, considerable research efforts have been directed at the design of adaptive flight control systems for the uncertain linear and nonlinear AHFV models [10-15].

A simplified control law is achieved by using a Dynamic Surface Control (DSC) technique [7-9], which suggests using a low pass filter at each design step of the backstepping technique, to avoid the derivative of the nonlinear functions. Using assumptions in the model, a DSC based fuzzy adaptive control scheme for a strict feedback system has been proposed by [15]. It has been shown that all the signals in the closed loop system are semiglobally uniformly bounded and the tracking error is minimized by a proper selection of controller parameters.

In this paper, the uncertain nonlinear mathematical model of AHFV is transformed to a pure feedback form. Air speed control is achieved by using a PI (Proportional Integral) controller and altitude tracking control is achieved by using a DSC based controller design procedure. Radial Basis Function (RBF) neural networks are used to approximate the smooth nonlinear functions that include the parameter uncertainties. First the design of a DSC controller is proposed for the case where complete states are available for measurement. Subsequently, the difficult to measure states are observed by a sliding mode observer. Simulation of the nonlinear closed loop AHFV system demonstrates the performance and robustness of the designed controller.

III. VEHICLE MODEL

The differential equations describing velocity, altitude, flight path angle, angle of attack and pitch rate of a model developed by NASA Langley research centre (1)-(5), for an AHFV are:

$$\dot{V} = \frac{T\cos\alpha - D}{m} - \frac{\mu\sin\gamma}{r^2}, \tag{1}$$

$$\dot{h} = V\sin\gamma, \tag{2}$$

$$\dot{\gamma} = \frac{L + T\sin\alpha}{mV} - \frac{(\mu - V^2 r)}{Vr^2}\cos\gamma, \tag{3}$$

$$\dot{\alpha} = q - \dot{\gamma}, \tag{4}$$

$$\dot{q} = M_{yy}/I_{yy}. \tag{5}$$

where

$$D = \frac{1}{2}\rho V^2 S C_D, \tag{6}$$

$$L = \frac{1}{2}\rho V^2 S C_L, \tag{7}$$

$$T = \frac{1}{2}\rho V^2 S C_T, \tag{8}$$

$$M_{yy} = \frac{1}{2}\rho V^2 S\bar{c}[C_M(\alpha) + C_M(\delta_E) + C_M(q)], \tag{9}$$

$$r = h + R_E. \tag{10}$$

A second order system is used to represent the engine dynamics as,

$$\ddot{\beta} = -2\xi\omega_n\dot{\beta} - \omega_n^2\beta + \omega_n^2\beta_c. \tag{11}$$

The nominal flight of the vehicle is at a trimmed cruise condition (Mach=15, V=15,060 ft/s, h =110,000ft, γ=0 deg and q=0 deg/sec, α=0.0312 rad, δ_E=-0.00695 rad, β=0.1762)[1]. The

uncertainty in the AHFV model is considered as an additive perturbation Δ in the parameters. Aerodynamic parameters and uncertainties (values given in Table. I) are defined as:

$$C_L = 0.6203\alpha, \tag{12}$$

$$C_D = 0.6450\alpha^2 + 0.0043378\alpha + 0.003772, \tag{13}$$

$$C_T = \begin{cases} 0.022576\beta & if \quad \beta < 1, \\ 0.0224 + 0.00336\beta & if \quad \beta > 1, \end{cases} \tag{14}$$

$$C_M(\alpha) = -0.035\alpha^2 + 0.036617(1 + \Delta C_{M\alpha})\alpha + 5.3261 \times 10^{-6}, \tag{15}$$

$$C_M(q) = (\bar{c}/2V)q(-6.796\alpha^2 + 0.3015\alpha - 0.2289), \tag{16}$$

$$C_M(\delta_E) = c_e(\delta_E - \alpha), \tag{17}$$

$$m = m_0(1 + \Delta m), \tag{18}$$

$$I_{yy} = I_0(1 + \Delta I), \tag{19}$$

$$S = S_0(1 + \Delta S), \tag{20}$$

$$\bar{c} = \bar{c}_0(1 + \Delta\bar{c}), \tag{21}$$

$$\rho = \rho_0(1 + \Delta\rho), \tag{22}$$

$$c_e = 0.0292(1 + \Delta c_e), \tag{23}$$

where the nominal values of the uncertain parameters are given by $m_0 = 9375$, $I_0 = 7 \times 10^6$, $S_0 = 3603$, $\bar{c}_0 = 80$, and $\rho_0 = 0.24325 \times 10^{-4}$.

Table 1. Uncertainty bounds

Uncertain parameter	Maximum additive uncertain value	
m	$\lvert\Delta m\rvert$	$\leq$ 0.03
I_{yy}	$\lvert\Delta I\rvert$	$\leq$ 0.02
S	$\lvert\Delta S\rvert$	$\leq$ 0.01
$\bar{c}$	$\lvert\Delta\bar{c}\rvert$	$\leq$ 0.01
ρ	$\lvert\Delta\rho\rvert$	$\leq$ 0.06
c_e	$\lvert\Delta c_e\rvert$	$\leq$ 0.03
$C_{M\alpha}$	$\lvert\Delta C_{M\alpha}\rvert$	$\leq$ 0.1

It can be inferred from the flight vehicle model (1)-(5), that air speed is mainly affected by throttle setting β_c and elevator deflection δ_E has a dominant contribution towards the altitude change, thus entailing a natural choice of input/output pairings for control design. For air speed control, a PI controller is designed to maintain the flight vehicle speed in the neighborhood of the

demanded air speed. Also, using flight vehicle model (2)-(5), a DSC based robust neural networks adaptive controller is designed for tracking the altitude demand. The effect of change in the air speed due to elevator deflection and the change in lift due to throttle setting can be viewed as a disturbance, that is compensated by the respective controllers. Tuning of the PI controller is carried out by improving the closed loop performance of the engine dynamics (11) and system dynamics (1) of the AHFV model. Altitude tracking can be achieved by generating the flight path angle demand as [15]

$$\gamma_d = \arcsin[-k_{hf}(h - h_d)/V], \tag{24}$$

where $k_{hf} > 0$ is a design parameter, used to set the rise time of the altitude tracking trajectory. We know that θ_p is related to γ and α by $\theta_p = \alpha + \gamma$. Using the state variables γ, θ_p, q and V, the pure feedback equations of the AHFV with uncertainties can then be written as

$$\begin{aligned}
\dot{\gamma} &= f_{10}(\gamma, \theta_p, V) + g_{10}(V)\theta_p + \Delta f_1(\gamma, \theta_p, V) + \Delta g_1(V)\theta_p,\\
\dot{\theta}_p &= q,\\
\dot{q} &= f_{30}(\gamma, \theta_p, q, V) + g_{30}(V)\delta_E + \Delta f_3(\gamma, \theta_p, q, V) + \Delta g_3(V)\delta_E,\\
y &= \gamma,
\end{aligned} \tag{25}$$

define

$$\begin{aligned}
f_1(\gamma, \theta_p, V) &= f_{10}(\gamma, \theta_p, V) + \Delta f_1(\gamma, \theta_p, V),\\
g_1(V)\theta_p &= g_{10}(V)\theta_p + \Delta g_1(V)\theta_p,\\
f_3(\gamma, \theta_p, q, V) &= f_{30}(\gamma, \theta_p, q, V) + \Delta f_3(\gamma, \theta_p, q, V),\\
g_3(V)\delta_E &= g_{30}(V)\delta_E + \Delta g_3(V)\delta_E,
\end{aligned} \tag{26}$$

where

$$\begin{aligned}
f_1(\gamma, \theta_p, V) &= \rho VS/2m[C_T(\sin\theta_p - \sin\gamma) - 0.6203\ \gamma\ ] - \tfrac{(\mu - V^2 r)}{V\ r^2}\cos\gamma,\\
g_1(V) &= 0.6203\ \rho VS/2m,\\
f_3(\gamma, \theta_p, q, V) &= \rho V^2 S\bar{c})/2I_{yy}[5.3261 \times 10^{-6} + 0.036617(1 + \Delta C_{M(\theta_p - \gamma)}(\theta_p - \gamma))\\
&\quad -c_e(\theta_p - \gamma)) - 0.035(\theta_p - \gamma)^2 + \bar{c}q/2V\ (-6.796(\theta_p - \gamma)^2\\
&\quad +0.3015(\theta_p - \gamma) - 0.2289)],\\
g_3(V) &= (\rho V^2 S\ \bar{c}\ c_e)/2I_{yy}.
\end{aligned}$$

Assumption 1: $f_1(\gamma, \theta_p, V), f_3(\gamma, \theta_p, q, V)$, $g_1(V)$ and $g_3(V)$ are unknown smooth functions. The virtual control gain function $g_1(.)$ and the actual control gain function $g_3(.)$ are strictly

positive. We assume that there exist positive constants $\overline{g}_i, \underline{g}_i$, such that $\overline{g}_i \geq g_i(.) \geq \underline{g}_i > 0,\ i = 1,3$.

Assumption 2: There exists constants $g_{ic} > 0$, such that, $|\dot{g}_i(.)| \leq g_{ic}, i = 1,3$.

Assumption 3: The reference signal (or altitude reference trajectory) and its derivatives are smooth bounded functions; $[y_r, \dot{y}_r, \ddot{y}_r]$ and thus $[\gamma_d, \dot{\gamma}_d, \ddot{\gamma}_d]$ belong to a known compact set for all $t \geq 0$.

IV. NONLINEAR CONTROLLER DESIGN

In this section a DSC based nonlinear robust neural networks adaptive controller is designed for the flight path angle tracking of the nonlinear generic AHFV, in order to achieve altitude tracking. It is assumed that V, h, q, α and γ are available for measurement.

RBF neural networks are used to approximate the unknown smooth nonlinear functions since they have an inherent property to approximate continuous functions to an arbitrary accuracy. RBF neural networks are of the general form $\theta^T \xi(x)$, where $\theta \in R^N$ is a vector of adjustable weights and $\xi(x) \in R^N$ is a vector of Gaussian basis functions. We denote the components of $\xi(x)$ by $\psi_j(x), j = 1, \ldots, N$. A commonly used Gaussian function is of the following form:

$$\psi_j(x) = \frac{1}{\sqrt{2\pi}\sigma} \exp\left(-\frac{\|x-\zeta_j\|^2}{2\sigma^2}\right),\ \sigma > 0, j = 1, \ldots, N, \tag{27}$$

where $\zeta_j \in R^N, j = 1, \ldots, N$, are constant vectors called the centre of the basis function and σ is a real number called the width of the basis function. According to the approximation property of the RBF networks [16], given a continuous real valued function $f: \Omega \to R$ with $\Omega \in R^n$ a compact set and any $\delta_m > 0$, by appropriately choosing $\sigma, \zeta_j \in R^n, j = 1, \ldots, N$, for some sufficiently large integer N, there exists an ideal weight vector $\theta^* \in R^N$ such that the RBF network $\theta^{*^T} \xi(x)$ can approximate the given function f with the approximation error bounded by δ_m , i.e.,

$$f(x) = \theta^{*^T} \xi(x) + \delta^*, \quad x \in \Omega, \tag{28}$$

with $|\delta^*| \leq \delta_m$, where δ^* represents the network reconstruction error, i.e.,

$$\delta^* = f(x) - \theta^{*^T} \xi(x). \tag{29}$$

Since θ^* is unknown, we need to estimate θ^* online. The estimate of θ^* will be denoted by $\hat{\theta}$.

We now proceed with a recursive DSC design procedure to form virtual control signals at step 1 and step 2 and actual control at step 3.

Step 1: The first surface error is

$$S_1 = \gamma - y_r, \tag{30}$$

whose derivative is

$$\dot{S}_1 = \dot{\gamma} - \dot{y}_r. \tag{31}$$

From (25) and (26), the above equation can be written as

$$\begin{aligned} \dot{S}_1 &= f_1(\gamma, \theta_p, V) + g_1(V)\theta_p - \dot{y}_r, \\ &= g_1(V)[g_1^{-1}(V)f_1(\gamma, \theta_p, V) + \theta_p - g_1^{-1}(V)\dot{y}_r]. \end{aligned} \tag{32}$$

We use neural networks to approximate

$$g_1^{-1}(V)\ f_1(\gamma, \theta_p, V) = \theta_{gf1}^{*T}\xi_{gf1}(\gamma, \theta_p, V) + \delta_{gf1}^{*}, \tag{33}$$

$$g_1^{-1}(V) = \theta_{g1}^{*T}\xi_{g1}(V) + \delta_{g1}^{*}. \tag{34}$$

Choose a virtual control signal

$$\overline{x}_2 = \bar{\theta}_p = -\hat{\theta}_{gf1}^{T}\xi_{gf1}(\gamma, \theta_p, V) + \hat{\theta}_{g1}^{T}\xi_{g1}(V)\dot{y}_r - \alpha_1 S_1, \tag{35}$$

where α_1 is a positive real constant, $\hat{\theta}_{gf1}^{T}$and $\hat{\theta}_{g1}^{T}$, are the estimates of $\theta_{gf1}^{*T}$and θ_{g1}^{*T}, respectively, and are updated as follows

$$\dot{\hat{\theta}}_{gf1} = \Gamma_{gf1}S_1\xi_{gf1}(\gamma, \theta_p, V) - \Gamma_{gf1}\eta_1\hat{\theta}_{gf1}, \tag{36}$$

$$\dot{\hat{\theta}}_{g1} = -\Gamma_{g1}S_1\xi_{g1}(V)\dot{y}_r - \Gamma_{g1}\eta_2\hat{\theta}_{g1}. \tag{37}$$

Let $\overline{x}_2$ pass through a first order filter with time constant τ_2 to obtain a new state variable z_2

$$\tau_2\dot{z}_2 + z_2 = \overline{x}_2, \quad z_2(0) = \overline{x}_2(0). \tag{38}$$

Step 2: The second surface error is

$$S_2 = \theta_p - z_2, \tag{39}$$

whose derivative is

$$\dot{S}_2 = \dot{\theta}_p - \dot{z}_2 = q - \dot{z}_2. \tag{40}$$

Choose a virtual control signal

$$\overline{x}_3 = \bar{q} = -\alpha_2 S_2 + \dot{z}_2, \tag{41}$$

where α_2 is a positive real constant. Let $\overline{x}_3$ pass through a first order filter with time constant τ_3 to obtain a new state variable z_3.

$$\tau_3\dot{z}_3 + z_3 = \overline{x}_3, \quad z_3(0) = \overline{x}_3(0). \tag{42}$$

Step 3: The third surface error is

$$S_3 = q - z_3, \tag{43}$$

whose derivative is

$$\dot{S}_3 = \dot{q} - \dot{z}_3. \tag{44}$$

From (25) and (26), the above equation can be written as

$$\dot{S}_3 = g_3(V)[g_3^{-1}(V)f_3(\gamma, \theta_p, q, V) + \delta_E - g_3^{-1}(V)\dot{z}_3], \tag{45}$$

we use neural networks to approximate

$$g_3^{-1}(V)\ f_3(\gamma, \theta_p, q, V) = \theta_{gf3}^{*T}\xi_{gf3}(\gamma, \theta_p, q, V) + \delta_{gf3}^{*}, \tag{46}$$

$$g_3^{-1}(V) = \theta_{g3}^{*T}\xi_{g3}(V) + \delta_{g3}^{*}. \tag{47}$$

Choose the final control signal as

$$\delta_E = -\hat{\theta}_{gf3}^{T}\xi_{gf3}(\gamma, \theta_p, q, V) + \hat{\theta}_{g3}^{T}\xi_{g3}(V)\dot{z}_3 - \alpha_3 S_3, \tag{48}$$

where α_3 is a positive real constant, $\hat{\theta}_{gf3}^{T}$and $\hat{\theta}_{g3}^{T}$, are the estimates of θ_{gf3}^{*T} and θ_{g3}^{*T}, respectively, and are updated as follows

$$\dot{\hat{\theta}}_{gf3} = \Gamma_{gf3}S_3\xi_{gf3}(\gamma, \theta_p, q, V) - \Gamma_{gf3}\eta_3\hat{\theta}_{gf3}, \tag{49}$$

$$\dot{\hat{\theta}}_{g3} = -\Gamma_{g3}S_3\xi_{g3}(V)\dot{z}_3 - \Gamma_{g3}\eta_4\hat{\theta}_{g3}. \tag{50}$$

V. STABILITY ANALYSIS

In this section we show that the control law and update law developed in the design procedure guarantee the uniform ultimate boundedness of all the signals in the closed loop system.

Define the estimation error as

$$\tilde{\theta} = \hat{\theta} - \theta^{*}, \tag{51}$$

also define the following errors

$$y_i = z_i - \overline{x}_i,\ i = 2,3. \tag{52}$$

Using (38) and (42), it follows that

$$\dot{z}_i = (\overline{x}_i - z_i)/\tau_i = -y_i/\tau_i, i = 2,3. \tag{53}$$

Then the closed-loop system in the new coordinates can be expressed as follows:

$$\dot{S}_1 = g_1(V)[S_2 - \alpha_1 S_1 - \tilde{\theta}_{gf1}^{T}\xi_{gf1}(\gamma, \theta_p, V) + \tilde{\theta}_{g1}^{T}\xi_{g1}(V)\dot{y}_r + \delta_{gf1}^{*} - \delta_{g1}^{*}\dot{y}_r + y_2], \tag{54}$$

$$\dot{S}_2 = S_3 - \alpha_2 S_2 + y_3, \tag{55}$$

$$\dot{S}_3 = g_3(V)[-\alpha_3 S_3 - \tilde{\theta}_{gf3}^T \xi_{gf3}(\gamma, \theta_p, q, V) + \tilde{\theta}_{g3}^T \xi_{g3}(V)\dot{z}_3 + \delta_{gf3}^* - \delta_{g3}^* \dot{z}_3], \tag{56}$$

$$\dot{y}_2 = -\frac{y_2}{\tau_2} + B_2(S_1, S_2, y_2, \tilde{\theta}_{gf1}, \tilde{\theta}_{g1}, y_r, \dot{y}_r, \ddot{y}_r), \tag{57}$$

$$\dot{y}_3 = -\frac{y_3}{\tau_3} + B_3(S_1, S_2, S_3, y_2, y_3, \tilde{\theta}_{gf1}, \tilde{\theta}_{g1}, \tilde{\theta}_{gf3}, \tilde{\theta}_{g3}, y_r, \dot{y}_r, \ddot{y}_r), \tag{58}$$

where

$$B_2(.) = \alpha_1 \dot{S}_1 + \dot{\hat{\theta}}_{gf1}^T \xi_{gf1}(\gamma, \theta_p, V) + \hat{\theta}_{gf1}^T \frac{\partial \xi_{gf1}(\gamma, \theta_p, V)}{\partial \gamma}\dot{\gamma} + \hat{\theta}_{gf1}^T \frac{\partial \xi_{gf1}(\gamma, \theta_p, V)}{\partial \theta_p}\dot{\theta}_p$$
$$+\hat{\theta}_{gf1}^T \frac{\partial \xi_{gf1}(\gamma, \theta_p, V)}{\partial V}\dot{V} - \dot{\hat{\theta}}_{g1}^T \xi_{g1}(V)\dot{y}_r - \hat{\theta}_{g1}^T \frac{\partial \xi_{g1}(V)}{\partial V}\dot{V}\dot{y}_r - \hat{\theta}_{g1}^T \xi_{g1}(V)\ddot{y}_r,$$

$$B_3(.) = \alpha_2 \dot{S}_2 + \frac{\dot{y}_2}{\tau_2},$$

are continuous functions.

Theorem 1: Consider the Lyapunov function candidate

$$\bar{V} := \sum_{i=1}^{3} V_i, \tag{59}$$

with

$$V_1 = \frac{1}{2}\frac{S_1^2}{g_1} + \frac{1}{2}y_2^2 + \frac{1}{2}\tilde{\theta}_{gf1}^T \Gamma_{gf1}^{-1} \tilde{\theta}_{gf1} + \frac{1}{2}\tilde{\theta}_{g1}^T \Gamma_{g1}^{-1} \tilde{\theta}_{g1}, \tag{60}$$

$$V_2 = \frac{1}{2}S_2^2 + \frac{1}{2}y_3^2, \tag{61}$$

$$V_3 = \frac{1}{2}\frac{S_3^2}{g_3} + \frac{1}{2}\tilde{\theta}_{gf3}^T \Gamma_{gf3}^{-1} \tilde{\theta}_{gf3} + \frac{1}{2}\tilde{\theta}_{g3}^T \Gamma_{g3}^{-1} \tilde{\theta}_{g3}, \tag{62}$$

where $\Gamma_{(.)} = \Gamma_{(.)}^T > 0$ is given by (36), (37), (49) and (50). Given a positive number κ, for all initial conditions of (59) satisfying

$$\bar{V}(0) := \sum_{i=1}^{3} V_i(0) \leq \kappa, \tag{63}$$

there exist $\alpha_i (i = 1,2,3), \tau_i (i = 2,3), \eta_i (i = 1, \ldots, 4), and \quad \Gamma_{(.)}$, such that all signals of (59) are uniformly ultimately bounded, and the tracking error converges to a residual set that can be made arbitrarily small by properly choosing the design parameters.

Proof: Taking time derivative of V_1, we have

$$\dot{V}_1 = \frac{S_1 \dot{S}_1}{g_1} - \frac{\dot{g}_1 S_1^2}{2g_1^2} + y_2 \dot{y}_2 + \tilde{\theta}_{gf1}^T \Gamma_{gf1}^{-1} \dot{\hat{\theta}}_{gf1} + \tilde{\theta}_{g1}^T \Gamma_{g1}^{-1} \dot{\hat{\theta}}_{g1}. \tag{64}$$

From (57) and (58) we have

$$\dot{y}_i = \frac{-y_i}{\tau_i} + B_i(.), \; i = 2,3,$$

from which we can obtain

$$\left|\dot{y}_i + \frac{y_i}{\tau_i}\right| \leq B_i(.),\ i = 2,3.$$

Hence

$$y_i\ \dot{y}_i \leq \frac{-y_i^2}{\tau_i} + B_i|y_i|,\ i = 2,3. \tag{65}$$

Using (65) and substituting update law (36) and (37) in (64), we have

$$\dot{V}_1 \leq -(\alpha_1 + \frac{\dot{g}_1}{2g_1^2})S_1^2 + S_1S_2 + S_1y_2 + S_1(\delta_{gf1}^* - \delta_{g1}^*\dot{y}_r) - \tilde{\theta}_{gf1}^T\eta_1\hat{\theta}_{gf1}$$
$$-\tilde{\theta}_{g1}^T\eta_2\hat{\theta}_{g1} - \frac{y_2^2}{\tau_2} + |y_2|B_2. \tag{66}$$

Define $\delta_1^* = \delta_{gf1}^* - \delta_{g1}^*\dot{y}_r$ (reconstruction error) and let $\delta_1^M > 0$ such that $|\delta_1^*| < \delta_1^M$. Therefore,

$$\dot{V}_1 \leq -(\alpha_1 + \frac{\dot{g}_1}{2g_1^2})S_1^2 + S_1S_2 + S_1y_2 + S_1\delta_1^* - \tilde{\theta}_{gf1}^T\eta_1\hat{\theta}_{gf1} - \tilde{\theta}_{g1}^T\eta_2\hat{\theta}_{g1} - \frac{y_2^2}{\tau_2} + |y_2|B_2. \tag{67}$$

Define compact sets

$$\Omega_1 := \{(y_r, \dot{y}_r, \ddot{y}_r): y_r^2 + \dot{y}_r^2 + \ddot{y}_r^2 \leq R_o\}, \tag{68}$$

$$\Omega_2 := \left\{\frac{S_1^2}{g_1} + S_2^2 + \frac{S_3^2}{g_3} + \sum_{j=2}^{3} y_j^2 + \tilde{\theta}_{gf1}^T\Gamma_{gf1}^{-1}\tilde{\theta}_{gf1} + \tilde{\theta}_{g1}^T\Gamma_{g1}^{-1}\tilde{\theta}_{g1}\right.$$
$$\left. + \tilde{\theta}_{gf3}^T\Gamma_{gf3}^{-1}\tilde{\theta}_{gf3} + \tilde{\theta}_{g3}^T\Gamma_{g3}^{-1}\tilde{\theta}_{g3} \leq 2\kappa,\right\} \tag{69}$$

where R_o can be determined from assumption 3. Note that $\Omega_1 \times \Omega_2$ is also compact and therefore, the continuous functions $|B_2|$ and $|B_3|$ have maximums on $\Omega_1 \times \Omega_2$, say $B_2 \leq M_2,\ B_3 \leq M_3$ with $M_2, M_3 > 0$. Also note that,

$$-\eta\tilde{\theta}_a^T\hat{\theta}_a \leq \frac{-\eta}{2}(\left\|\tilde{\theta}_a\right\|^2 - \|\theta_a\|^2), \tag{70}$$

$$|y_i|B_i \leq \frac{1}{2}y_i^2 + \frac{1}{2}B_i^2 \leq \frac{1}{2}y_i^2 + \frac{1}{2}M_i^2,\ i = 2,3. \tag{71}$$

Hence, (67) satisfies

$$\dot{V}_1 \leq -(\alpha_1 - \frac{g_{1c}}{2g_1^2} - \frac{3}{2})S_1^2 + \frac{S_2^2}{2} - (\frac{1}{\tau_2} + 1)y_2^2 + \frac{M_2^2}{2} + \frac{\delta_1^{*2}}{2} - \frac{\eta_1}{2}\left\|\tilde{\theta}_{gf1}\right\|^2 + \frac{\eta_1}{2}\left\|\theta_{gf1}\right\|^2$$
$$-\frac{\eta_2}{2}\left\|\tilde{\theta}_{g1}\right\|^2 + \frac{\eta_2}{2}\left\|\theta_{g1}\right\|^2,$$
$$\leq -(\alpha_1 - \frac{g_{1c}}{2g_1^2} - \frac{3}{2})S_1^2 + \frac{S_2^2}{2} - (\frac{1}{\tau_2} + 1)y_2^2 + \frac{M_2^2}{2} + \frac{\delta_1^{M^2}}{2} - \frac{\eta_1}{2\lambda_{\max}\Gamma_{gf1}^{-1}}\tilde{\theta}_{gf1}^T\Gamma_{gf1}^{-1}\tilde{\theta}_{gf1} + \frac{\eta_1}{2}\left\|\theta_{gf1}\right\|^2$$
$$-\frac{\eta_2}{2\lambda_{\max}\Gamma_{g1}^{-1}}\tilde{\theta}_{g1}^T\Gamma_{g1}^{-1}\tilde{\theta}_{g1} + \frac{\eta_2}{2}\left\|\theta_{g1}\right\|^2,$$

$$\leq -\gamma_1[\frac{1}{g_1(V)}S_1^2 + \tilde{\theta}_{gf1}^{T}\Gamma_{gf1}^{-1}\tilde{\theta}_{gf1} + \tilde{\theta}_{g1}^{T}\Gamma_{g1}^{-1}\tilde{\theta}_{g1} + y_2^2] + C_1 + \frac{S_2^2}{2},$$

$$\leq -2\gamma_1 V_1 + C_1 + S_2^2/2, \tag{72}$$

where $\lambda_{\max}(.)$ is the maximum eigenvalue of $(.)$ and

$$0 < \gamma_1 < min[k_1, \frac{\eta_1}{2\lambda_{\max}\Gamma_{gf1}^{-1}}, \frac{\eta_2}{2\lambda_{\max}\Gamma_{g1}^{-1}}, \frac{1}{\tau_2} + 1],$$

$$k_1 = (\alpha_1 - \frac{g_{1c}}{2g_1^2} - \frac{3}{2})\underline{g_1} > 0,$$

$$C_1 = \frac{M_2^2}{2} + \frac{\delta_1^{M^2}}{2} + \frac{\eta_1}{2}\left\|\theta_{gf1}\right\|^2 + \frac{\eta_2}{2}\left\|\theta_{g1}\right\|^2.$$

Similarly

$$\dot{V}_2 \leq -(\alpha_2 - \frac{3}{2})S_2^2 - \frac{S_2^2}{2} - (\frac{1}{\tau_3} - 1)y_3^2 + \frac{M_3^2}{2} + \frac{S_3^2}{2},$$

$$\leq -\gamma_2(S_2^2 + y_3^2) + C_2 - \frac{S_2^2}{2} + \frac{S_3^2}{2},$$

$$\leq -2\gamma_2 V_2 + C_2 - \tfrac{S_2^2}{2} + \tfrac{S_3^2}{2}, \tag{73}$$

where $0 < \gamma_2 < min[k_2, \frac{1}{\tau_3} - 1], k_2 = (\alpha_2 - \frac{3}{2}) > 0, C_2 = \frac{M_3^2}{2}$.

Also define $\delta_3^* = \delta_{gf3}^* - \delta_{g3}^*\dot{z}_3$ (reconstruction error) and let $\delta_3^M > 0$ such that $|\delta_3^*| < \delta_3^M$. Therefore,

$$\dot{V}_3 \leq -(\alpha_3 - \tfrac{g_{3c}}{2g_3^2} + 1)S_3^2 + \tfrac{\delta_3^{M^2}}{2} - \tfrac{\eta_3}{2\lambda_{\max}\Gamma_{gf3}^{-1}}\tilde{\theta}_{gf3}^{T}\Gamma_{gf3}^{-1}\tilde{\theta}_{gf3} + \tfrac{\eta_3}{2}\left\|\theta_{gf3}\right\|^2$$

$$-\tfrac{\eta_4}{2\lambda_{\max}\Gamma_{g3}^{-1}}\tilde{\theta}_{g3}^{T}\Gamma_{g3}^{-1}\tilde{\theta}_{g3} + \tfrac{\eta_4}{2}\left\|\theta_{g3}\right\|^2 - \tfrac{S_3^2}{2},$$

$$\leq -\gamma_3[\tfrac{1}{g_3(V)}S_3^2 + \tilde{\theta}_{gf3}^{T}\Gamma_{gf3}^{-1}\tilde{\theta}_{gf3} + \tilde{\theta}_{g3}^{T}\Gamma_{g3}^{-1}\tilde{\theta}_{g3}] + C_3 - \tfrac{S_3^2}{2},$$

$$\leq -2\gamma_3 V_3 + C_3 - S_3^2/2, \tag{74}$$

where

$$0 < \gamma_3 < min[k_2, \tfrac{\eta_3}{2\lambda_{\max}\Gamma_{gf3}^{-1}}, \tfrac{\eta_4}{2\lambda_{\max}\Gamma_{g3}^{-1}}],$$

$$k_2 = (\alpha_3 - \tfrac{g_{3c}}{2g_3^2} + 1)\underline{g_3} > 0,$$

$$C_3 = \tfrac{\delta_3^{M^2}}{2} + \tfrac{\eta_3}{2}\left\|\theta_{gf3}\right\|^2 + \tfrac{\eta_4}{2}\left\|\theta_{g3}\right\|^2.$$

From (72), (73) and (74), we have

$$\dot{\bar{V}} = \sum_{i=1}^{3} \uparrow (V_i + C_i) \leq -2\varpi \bar{V} + C, \tag{75}$$

where $0 < \varpi < min[\gamma_1, \gamma_2, \gamma_3]$ and $C = \sum_{i=1}^{3} \uparrow C_i$. If $\bar{V} = \kappa$, then $\dot{\bar{V}} < 0$ when $\varpi > \frac{C}{2\kappa}$. That is, if $\bar{V}(0) \leq \kappa$, then $\bar{V}(t) \leq \kappa, \forall t \geq 0$, or in other words, $\bar{V} \leq \kappa$ is an invariant set. Moreover solving (75), we can obtain that

$$0 \leq \bar{V} \leq \frac{C}{2\varpi} + \left(\bar{V}(0) - \frac{C}{2\varpi}\right) e^{-2\varpi t}. \tag{76}$$

Furthermore,

$$\lim_{t \to \infty} \bar{V}(t) \leq \frac{C}{2\varpi}. \tag{77}$$

The inequality (77) shows that the tracking error S_1 given by (30) can converge to an arbitrarily small residual set by choosing ϖ sufficiently large, which can be done by properly choosing design parameters $\alpha_i (i = 1,2,3), \tau_i (i = 2,3), \eta_i (i = 1, \ldots, 4), and \quad \Gamma_{(.)}$.

VI. SLIDING MODE OBSERVER DESIGN

For a hypersonic air vehicle, flight path angle and angle of attack require costly sensors for measurement. In order to observe these angles, a sliding mode observer is designed by using the method developed by [17] and as applied to the same problem by [1]. The overall controller-observer closed loop system is shown in Figure 1.

The structure of the sliding mode observer is as given below[1]:

$$\dot{\hat{h}} = V \sin\hat{\gamma} + \eta_{1ob} \tilde{h} + k_h sat(\tilde{h}/\Phi_{\tilde{h}}), \tag{78}$$

$$\dot{\hat{q}} = \hat{M}_{yy}/I_{yy} + \eta_{2ob} \tilde{q} + k_q sat(\tilde{q}/\Phi_{\tilde{q}}), \tag{79}$$

$$\dot{\hat{\gamma}} = \frac{\hat{L} + T \sin\hat{\alpha}}{mV} - \frac{(\mu - V^2 r)}{Vr^2} \cos\hat{\gamma} + \eta_{3ob} \tilde{h} + k_\gamma sat(\tilde{h}/\Phi_{\tilde{h}}), \tag{80}$$

$$\dot{\hat{\alpha}} = \hat{q} - \dot{\hat{\gamma}} + \eta_{4ob} \tilde{q} + k_\alpha sat(\tilde{q}/\Phi_{\tilde{q}}), \tag{81}$$

where

$$\tilde{h} = h - \hat{h},$$

$$\tilde{q} = q - \hat{q},$$

$$\hat{L} = \frac{1}{2} \rho_0 V^2 S_0 \times 0.6203 \hat{\alpha},$$

$$\hat{M}_{yy} = \frac{1}{2} \rho_0 V^2 S_0 \bar{c}_0 [(-0.035\hat{\alpha}^2 + 0.036617\hat{\alpha} + 5.3261 \times 10^{-6}) + (\bar{c}_0/2V) q (-6.796\hat{\alpha}^2 + 0.3015\hat{\alpha} - 0.2289) + 0.0292(\delta_E - \hat{\alpha})],$$

$$sat(\tilde{e}/\Phi_{\tilde{e}}) = \begin{cases} 1 & \tilde{e}/\Phi_{\tilde{e}} > 1, \\ \tilde{e}/\Phi_{\tilde{e}} & |\ \tilde{e}/\Phi_{\tilde{e}}| \leq 1, \\ -1 & \tilde{e}/\Phi_{\tilde{e}} < -1. \end{cases}$$

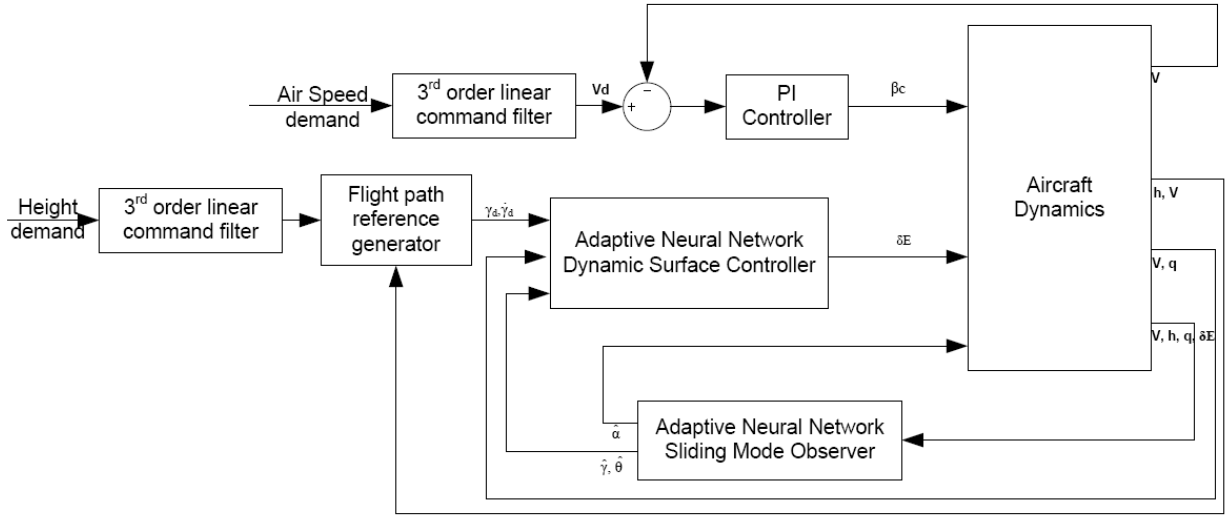

Figure 1. Overall Controller-Observer closed loop system.

In the observer (78)-(81), the values of $\eta_{1ob}, \eta_{2ob}, \eta_{3ob}, \eta_{4ob}$ are selected as 1.95, 1.5, 0.0001, 0.0082, respectively, and the sliding gains k_h, k_q, k_γ and k_α are chosen as per the design requirement[1]. A saturation function is used in the observer to smooth the discontinuity in the thin boundary layers $\Phi_{\tilde{h}} = 0.75$ and $\Phi_{\tilde{q}} = 1$, neighboring the switching surfaces. This methodology by virtue of its low pass filter structure helps in alleviating chattering phenomenon, but there is a trade off between tracking performance and robustness[18]. For the design of the sliding mode observer, V, h and q are assumed to be available for measurement. Therefore, the sliding manifold of the observer is defined by $S_0 = [\tilde{h} \quad \tilde{q}]^T = 0$. During sliding condition ($S_0 = \dot{S}_0 = 0$), the average error dynamics is given by, $\tilde{h} = 0$, $\tilde{q} = 0$. The observation error dynamics in altitude is given by

$$\dot{\tilde{h}} = \dot{h} - \dot{\hat{h}} = 0, \tag{82}$$

using (2) and (78), we have

$$k_h sat(\tilde{h}/\Phi_{\tilde{h}}) = V(\sin\gamma - \sin\hat{\gamma}), \tag{83}$$

also for pitch rate, the observation error dynamics is given by

$$\dot{\tilde{q}} = \dot{q} - \dot{\hat{q}} = 0, \tag{84}$$

using (5) and (79), we have

$$k_q sat(\tilde{q}/\Phi_{\tilde{q}}) = \frac{1}{2I_0}\rho_0 V^2 S_0 \bar{c}_0[-0.035(\alpha^2 - \hat{\alpha}^2) + 0.007417\tilde{\alpha} + (\bar{c}_0/2V)q(-6.796(\alpha^2 - \hat{\alpha}^2) + 0.3015\tilde{\alpha})], \quad (85)$$

observation error dynamics of the flight path angle is

$$\dot{\tilde{\gamma}} = \dot{\gamma} - \dot{\hat{\gamma}}, \quad (86)$$

using (3) and (80), we have

$$\dot{\tilde{\gamma}} = \frac{0.3101\ \rho_0 V^2 S_0(\alpha - \hat{\alpha}) + T(\sin\alpha - \sin\hat{\alpha})}{mV} - \frac{(\mu - V^2 r)(\cos\gamma - \cos\hat{\gamma})}{Vr^2} - k_\gamma sat(\tilde{h}/\Phi_{\tilde{h}}), \quad (87)$$

finally, observation error dynamics of the angle of attack is

$$\dot{\tilde{\alpha}} = \dot{\alpha} - \dot{\hat{\alpha}}, \quad (88)$$

using (4) and (81), we have

$$\dot{\tilde{\alpha}} = -\dot{\tilde{\gamma}} - k_\alpha sat(\tilde{q}/\Phi_{\tilde{q}}). \quad (89)$$

The velocity of a hypersonic flight vehicle is high, therefore, the term $(\bar{c}_0/2V)q \approx 0$. Also using small angle approximations, (83) can be written as

$$sat(\tilde{h}/\Phi_{\tilde{h}}) \approx \frac{V\tilde{\gamma}}{k_h}, \quad (90)$$

similarly from (85), we have

$$sat(\tilde{q}/\Phi_{\tilde{q}}) \approx \frac{1}{I_0 k_q}\rho_0 V^2 S_0 \bar{c}_0(0.003735\tilde{\alpha}), \quad (91)$$

substituting the value of $sat(\tilde{h}/\Phi_{\tilde{h}})$ from (90) in (87) and using small angle approximation, we have

$$\dot{\tilde{\gamma}} \approx \left(\frac{0.3101\ \rho_0 V^2 S_0 + T}{mV}\right)\tilde{\alpha} - \left(\frac{Vk_\gamma}{k_h}\right)\tilde{\gamma}, \quad (92)$$

substituting the value of $sat(\tilde{q}/\Phi_{\tilde{q}})$ from (91) in (89) and using (92), we have

$$\dot{\tilde{\alpha}} \approx \left(\frac{Vk_\gamma}{k_h}\right)\tilde{\gamma} - \left(\frac{0.3101\ \rho_0 V^2 S_0 + T}{mV}\right)\tilde{\alpha} - \frac{k_\alpha}{I_0 k_q}\rho_0 V^2 S_0 \bar{c}_0(0.003735\tilde{\alpha}). \quad (93)$$

Substituting trim conditions in equations (92) and (93), we have

$$\dot{\tilde{\gamma}} \approx -15060(k_\gamma/k_h)\tilde{\gamma} + 0.0439\tilde{\alpha}, \quad (94)$$

$$\dot{\tilde{\alpha}} \approx -[0.8485(k_\alpha/k_q) + 0.0439]\tilde{\alpha} + 15060(k_\gamma/k_h)\tilde{\gamma}. \quad (95)$$

We need to make the error dynamics of the observer on the sliding surface faster than the tracking error dynamics. If k_h, k_q, k_γ and k_α are selected as 1000, 0.1, 1 and 1.52, respectively, the poles of the reduced order error dynamics of (94) and (95) are placed at -15.06 and -12.6815, which makes the error dynamics of the observer fast enough.

The observer (78)-(81) can be written as follows:

$$\dot{\hat{h}} = \hat{f}_h(\hat{\gamma}, V) + \eta_{1ob}\tilde{h} + k_h sat(\tilde{h}/\Phi_{\tilde{h}}), \tag{96}$$

$$\dot{\hat{q}} = \hat{f}_{qc}(\hat{\gamma}, \hat{\theta}_p, q, \delta_E, V) + \eta_{2ob}\tilde{q} + k_q sat(\tilde{q}/\Phi_{\tilde{q}}), \tag{97}$$

$$\dot{\hat{\gamma}} = \hat{f}_{\gamma c}(\hat{\gamma}, \hat{\theta}_p, V) + \eta_{3ob}\tilde{h} + k_\gamma sat(\tilde{h}/\Phi_{\tilde{h}}), \tag{98}$$

$$\dot{\hat{\alpha}} = \hat{q} - \dot{\hat{\gamma}} + \eta_{4ob}\tilde{q} + k_\alpha sat(\tilde{q}/\Phi_{\tilde{q}}). \tag{99}$$

where, $\hat{f}_h(\hat{\gamma}, V) = V\sin\hat{\gamma}$, $\hat{f}_{qc}(\hat{\gamma}, \hat{\theta}_p, q, \delta_E, V) = \hat{M}_{yy}/I_{yy}$, $\hat{f}_{\gamma c}(\hat{\gamma}, \hat{\theta}_p, V) = \frac{\hat{L}+T\sin\hat{\alpha}}{mV} - \frac{(\mu - V^2 r)}{Vr^2}\cos\hat{\gamma}$.

Assumption 4: Let $\hat{f}_{qc}(\hat{\gamma}, \hat{\theta}_p, q, \delta_E, V)$ and $\hat{f}_{\gamma c}(\hat{\gamma}, \hat{\theta}_p, V)$ be unknown smooth functions.

Remark 1: Neural Networks will be used to approximate $\hat{f}_{qc}(\hat{\gamma}, \hat{\theta}_p, q, \delta_E, V)$ and $\hat{f}_{\gamma c}(\hat{\gamma}, \hat{\theta}_p, V)$. There is no need to approximate $\hat{f}_h(\hat{\gamma}, V)$, as V and $\hat{\gamma}$ may be used to form this nonlinear function.

Theorem 2: Let the system (25) have bounded input and let the state observer be of the form given by (78)-(81), then there exist positive constants $k_h, k_q, k_\gamma, k_\alpha, \eta_{iob}, i = 1,..,4$, such that the observer errors $\tilde{h}, \tilde{q}, \tilde{\gamma}$ and $\tilde{\alpha}$ approach zero in finite time.

Proof: Consider the error dynamics of the measured variable in height,

$$\dot{\tilde{h}} = \dot{h} - \dot{\hat{h}}, \tag{100}$$

using (2) and (78), we have

$$\dot{\tilde{h}} = -\tilde{f}_h(\gamma, V) - \eta_{1ob}\tilde{h} - k_h sat(\tilde{h}/\Phi_{\tilde{h}}). \tag{101}$$

Now consider the Lyapunov function

$$V_h = \frac{1}{2}\tilde{h}^2, \tag{102}$$

the derivative of which is given by

$$\dot{V}_h = \tilde{h}\dot{\tilde{h}}, \tag{103}$$

substituting the value of $\dot{\tilde{h}}$ from (101) in (103) we have

$$\dot{V}_h = \tilde{h}(-\tilde{f}_h(\gamma, V) - \eta_{1ob}\tilde{h} - k_h sat(\tilde{h}/\Phi_{\tilde{h}})), \tag{104}$$

which verifies the inequality $\dot{V}_h < 0$ when $\eta_{1ob}\tilde{h}^2 + k_h\tilde{h}\ sat(\tilde{h}/\Phi_{\tilde{h}})$ is chosen such that $\eta_{1ob}\tilde{h}^2 + k_h\tilde{h}sat(\tilde{h}/\Phi_{\tilde{h}}) > \left|\tilde{h}\ \tilde{f}_h(\gamma, V)\right|_{\max}$ (where $\left|\tilde{h}\tilde{f}_h(\gamma, V)\right|_{\max}$ denotes the maximum value of $\tilde{h}\ \tilde{f}_h(\gamma, V), \forall\ t \in 0, \infty$]). The decreasing Lyapunov funciton means that the sliding surface

$\tilde{h} = 0$ is achieved in finite time t_0(we have $\left|\tilde{h}\ \tilde{f}_h(\gamma, V)\right|_{\max} = \left|\tilde{h}\ \tilde{f}_h(\gamma, V)\right|_{\max}^{t_0}$ and $\left|\tilde{h}\ \tilde{f}_h(\gamma, V)\right|_{\max}^{t_0}$ is the maximum value of $\tilde{h}\ \tilde{f}_h(\gamma, V)$, $\forall\ t \in 0, t_0$])[19].

Now consider the error dynamics of the measured variable q

$$\dot{\tilde{q}} = \dot{q} - \dot{\hat{q}}, \tag{105}$$

using (5), (79) and the following

$$f_{qc}(\gamma, \theta_p, q, \delta_E, V) = \theta_{qc}^{*T} \xi_{qc}(\hat{\gamma}, \hat{\theta}_p, q, \delta_E, V) + \delta_{qc}^*, \tag{106}$$

where $f_{qc}(\gamma, \theta_p, q, \delta_E, V) = M_{yy}/I_{yy}$,

$$\hat{f}_{qc}(\hat{\gamma}, \hat{\theta}_p, q, \delta_E, V) = \hat{\theta}_{qc}^{T} \xi_{qc}(\hat{\gamma}, \hat{\theta}_p, q, \delta_E, V), \tag{107}$$

we have

$$\dot{\tilde{q}} = -\tilde{\theta}_{qc} \xi_{qc}(\hat{\gamma}, \hat{\theta}_p, q, \delta_E, V) + \delta_{qc}^* - \eta_{2ob} \tilde{q} - k_q sat(\tilde{q}/\Phi_{\tilde{q}}). \tag{108}$$

Consider the Lyapunov function

$$V_q = \frac{1}{2}\tilde{q}^2 + \frac{1}{2}\tilde{\theta}_{qc} \Gamma_{qc}^{-1} \tilde{\theta}_{qc}, \tag{109}$$

the derivative of which is

$$\dot{V}_q = \tilde{q}\dot{\tilde{q}} + \tilde{\theta}_{qc} \Gamma_{qc}^{-1} \dot{\hat{\theta}}_{qc}, \tag{110}$$

substituting the value of $\dot{\tilde{q}}$ from (108) in (110), we have

$$\dot{V}_q = \tilde{q}[-\tilde{\theta}_{qc} \xi_{qc}(\hat{\gamma}, \hat{\theta}_p, q, \delta_E, V) + \delta_{qc}^* - \eta_{2ob} \tilde{q} - k_q sat(\tilde{q}/\Phi_{\tilde{q}})] + \tilde{\theta}_{qc} \Gamma_{qc}^{-1} \dot{\hat{\theta}}_{qc}, \tag{111}$$

let the estimate $\hat{\theta}_{qc}^{T}$ of θ_{qc}^{*T} be updated as $\dot{\hat{\theta}}_{qc} = \Gamma_{qc} \tilde{q}\ \xi_{qc}(\hat{\gamma}, \hat{\theta}_p, q, \delta_E, V) - \Gamma_{qc} \eta_5 \hat{\theta}_{qc}$. Using $\dot{\hat{\theta}}_{qc}$ and (70), we have

$$\dot{V}_q \leq \tilde{q}(\delta_{qc}^* - \eta_{2ob} \tilde{q} - k_q sat(\tilde{q}/\Phi_{\tilde{q}})) - \frac{\eta_5}{2}\left\|\tilde{\theta}_{qc}\right\|^2 + \frac{\eta_5}{2}\left\|\theta_{qc}\right\|^2, \tag{112}$$

which verifies the inequality $\dot{V}_q < 0$ when $\eta_{2ob}\tilde{q}^2 + k_q\ \tilde{q}\ sat(\tilde{q}/\Phi_{\tilde{q}})$ is chosen such that $\eta_{2ob}\tilde{q}^2 + k_q\ \tilde{q}\ sat(\tilde{q}/\Phi_{\tilde{q}}) > \left|\tilde{q}\ \delta_{qc}^*\right|_{\max} + \left|\frac{\eta_5}{2}\left\|\theta_{qc}\right\|^2\right|_{\max}$(where $\left|\tilde{q}\ \delta_{qc}^*\right|_{\max} + \left|\frac{\eta_5}{2}\left\|\theta_{qc}\right\|^2\right|_{\max}$ denotes the maximum value of $\tilde{q}\ \delta_{qc}^* + \frac{\eta_5}{2}\left\|\theta_{qc}\right\|^2, \forall\ t \in 0, \infty$]). The decreasing Lyapunov funciton means that the sliding surface $\tilde{q} = 0$ is achieved in finite time t_1(we have $\left|\tilde{q}\ \delta_{qc}^*\right|_{\max} + \left|\frac{\eta_5}{2}\left\|\theta_{qc}\right\|^2\right|_{\max} = \left|\tilde{q}\ \delta_{qc}^*\right|_{\max}^{t_1} + \left|\frac{\eta_5}{2}\left\|\theta_{qc}\right\|^2\right|_{\max}^{t_1}$ and $\left|\tilde{q}\ \delta_{qc}^*\right|_{\max}^{t_1} + \left|\frac{\eta_5}{2}\left\|\theta_{qc}\right\|^2\right|_{\max}^{t_1}$ is the maximum value of $\tilde{q}\ \delta_{qc}^* + \frac{\eta_5}{2}\left\|\theta_{qc}\right\|^2, \forall\ t \in 0, t_1$]).

Consider now the error dynamics of the flight path angle

$$\dot{\tilde{\gamma}} = \dot{\gamma} - \dot{\hat{\gamma}}, \tag{113}$$

using (3), (80) and the following

$$f_{\gamma c}(\gamma, \theta_p, V) = \theta_{\gamma c}^{*T} \xi_{\gamma c}(\hat{\gamma}, \hat{\theta}_p, V) + \delta_{\gamma c}^{*}, \tag{114}$$

where $f_{\gamma c}(\gamma, \theta_p, V) = \frac{L+T\sin\alpha}{mV} - \frac{(\mu - V^2 r)}{Vr^2}\cos\gamma$,

$$\hat{f}_{\gamma c}(\hat{\gamma}, \hat{\theta}_p, V) = \hat{\theta}_{\gamma c}^{T} \xi_{\gamma c}(\hat{\gamma}, \hat{\theta}_p, V), \tag{115}$$

we have

$$\dot{\tilde{\gamma}} = -\tilde{\theta}_{\gamma c} \xi_{\gamma c}(\hat{\gamma}, \hat{\theta}_p, V) + \delta_{\gamma c}^{*} - \eta_{3ob}\tilde{h} - k_{\gamma} sat(\tilde{h}/\Phi_{\tilde{h}}). \tag{116}$$

Consider the Lyapunov function

$$V_{\gamma} = \frac{1}{2}\tilde{\gamma}^2 + \frac{1}{2}\tilde{\theta}_{\gamma c}\Gamma_{\gamma c}^{-1}\tilde{\theta}_{\gamma c}, \tag{117}$$

the derivative of which is

$$\dot{V}_{\gamma} = \tilde{\gamma}\dot{\tilde{\gamma}} + \tilde{\theta}_{\gamma c}\Gamma_{\gamma c}^{-1}\dot{\hat{\theta}}_{\gamma c}, \tag{118}$$

substituting the value of $\dot{\tilde{\gamma}}$ from (116), we have

$$\dot{V}_{\gamma} = \tilde{\gamma}[-\tilde{\theta}_{\gamma c}\xi_{\gamma c}(\hat{\gamma}, \hat{\theta}_p, V) + \delta_{\gamma c}^{*} - \eta_{3ob}\tilde{h} - k_{\gamma} sat(\tilde{h}/\Phi_{\tilde{h}})] + \tilde{\theta}_{\gamma c}\Gamma_{\gamma c}^{-1}\dot{\hat{\theta}}_{\gamma c}. \tag{119}$$

from (90), we have

$$\tilde{\gamma} \approx \frac{k_h}{V} sat(\tilde{h}/\Phi_{\tilde{h}}), \tag{120}$$

substituting (120) in (119) we have

$$\dot{V}_{\gamma} \approx \frac{k_h}{V} sat(\tilde{h}/\Phi_{\tilde{h}})[-\tilde{\theta}_{\gamma c}\xi_{\gamma c}(\hat{\gamma}, \hat{\theta}_p, V) + \delta_{\gamma c}^{*} - \eta_{3ob}\tilde{h} - k_{\gamma} sat(\tilde{h}/\Phi_{\tilde{h}})] + \tilde{\theta}_{\gamma c}\Gamma_{\gamma c}^{-1}\dot{\hat{\theta}}_{\gamma c}, \tag{121}$$

let the estimate $\hat{\theta}_{\gamma c}^{T}$ of $\theta_{\gamma c}^{*T}$ be updated as $\dot{\hat{\theta}}_{\gamma c} = \Gamma_{\gamma c}\ \frac{k_h}{V} sat(\tilde{h}/\Phi_{\tilde{h}})\ \xi_{\gamma c}(\hat{\gamma}, \hat{\theta}_p, V) - \Gamma_{\gamma c}\eta_6\hat{\theta}_{\gamma c}$.

Using $\dot{\hat{\theta}}_{\gamma c}$ and (70), we have

$$\dot{V}_{\gamma} \leq \frac{k_h}{V} sat(\tilde{h}/\Phi_{\tilde{h}})[\delta_{\gamma c}^{*} - \eta_{3ob}\tilde{h} - k_{\gamma} sat(\tilde{h}/\Phi_{\tilde{h}})] - \frac{\eta_6}{2}\left\|\tilde{\theta}_{\gamma c}\right\|^2 + \frac{\eta_6}{2}\left\|\theta_{\gamma c}\right\|^2. \tag{122}$$

Similar to (104), the system is finite time stable if $\frac{k_h}{V} sat(\tilde{h}/\Phi_{\tilde{h}})[\eta_{3ob}\tilde{h} + k_{\gamma} sat(\tilde{h}/\Phi_{\tilde{h}})] > \left|\frac{k_h}{V} sat(\tilde{h}/\Phi_{\tilde{h}})\ \delta_{\gamma c}^{*}\right|_{\max} + \left|\frac{\eta_6}{2}\left\|\theta_{\gamma c}\right\|^2\right|_{\max}$ for all $t > t_2$ and some $t_2 > t_0$.

Finally consider the error dynamics of the angle of attack

$$\dot{\tilde{\alpha}} = \dot{\alpha} - \dot{\hat{\alpha}}, \tag{123}$$

using (4) and (99), we have

$$\dot{\tilde{\alpha}} = \tilde{q} - \dot{\tilde{\gamma}} - \eta_{4ob}\tilde{q} - k_{\alpha} sat(\tilde{q}/\Phi_{\tilde{q}}). \tag{124}$$

Also consider the Lyapunov function

$$V_\alpha = \frac{1}{2}\tilde{\alpha}^2, \tag{125}$$

the derivative of which is

$$\dot{V}_\alpha = \tilde{\alpha}\dot{\tilde{\alpha}}, \tag{126}$$

substituting the value of $\dot{\tilde{\alpha}}$ from (124), we have

$$\dot{V}_\alpha = \tilde{\alpha}[\tilde{q} - \dot{\hat{\gamma}} - \eta_{4ob}\tilde{q} - k_\alpha sat(\tilde{q}/\Phi_{\tilde{q}})]. \tag{127}$$

From (91), we have

$$\tilde{\alpha} \approx Q\ sat(\tilde{q}/\Phi_{\tilde{q}}), \tag{128}$$

where $Q = k_q I_0/(0.003735\ \rho_0 V^2 S_0 \bar{c}_0)$, substituting (128) in (127) we have

$$\dot{V}_\alpha \approx Q\ sat(\tilde{q}/\Phi_{\tilde{q}})[\tilde{q} - \dot{\hat{\gamma}} - \eta_{4ob}\tilde{q} - k_\alpha sat(\tilde{q}/\Phi_{\tilde{q}})]. \tag{129}$$

Similar to (112), the system is finite time stable if $\eta_{4ob}\tilde{q} + k_\alpha sat(\tilde{q}/\Phi_{\tilde{q}}) > \left|\tilde{q} - \dot{\hat{\gamma}}\right|_{\max}$ for all $t > t_3$ and some $t_3 > t_1$.

VII. NUMERICAL SIMULATION

a. DSC design without observer

Numerical simulation of the nonlinear AHFV is conducted to verify the effectiveness of the closed loop performance of the control system at trimmed cruise conditions of 110,000 ft and Mach 15. Performance of the controller designed in section IV is ascertained by a step change of 100 ft/s in airspeed and 2000 ft in altitude for both the nominal and uncertain vehicle model. In order to obtain differentiable commands satisfying assumption 3, a third order linear command filter $\left(\frac{0.125}{(s+0.5)^3}\right)$ is used for the altitude demand, smoothing of the air speed demand is also carried out by passing it through a third order linear command filter $\left(\frac{1}{(s+1)^3}\right)$.

The controller parameters chosen for the simulation are: PI controller gains (Proportional gain 0.6, Integral gain 0.8), and DSC parameters are $\alpha_1 = 10,\ \alpha_2 = 3,\ \alpha_3 = 2,\ \{\tau_2, \tau_3 = 0.005\}$. For the approximation of the nonlinear functions, parameters of the update law along with centres $\zeta_{(.)}$ and widths $\sigma_{(.)}$ of the basis functions of RBF neural networks are to be selected. The nonlinear functions $g_1^{-1}(V)\ f_1(\gamma, \theta_p, V), g_1^{-1}(V), g_3^{-1}(V)\ f_3(\gamma, \theta_p, q, V)$ and $g_3^{-1}(V)$ are approximated with centers evenly spaced in $\zeta_{gf1} \in [-1,1] \times [-1,1] \times [-1,1],\ \zeta_{g1} \in [-3,3],\ \zeta_{gf3} \in [-1,1] \times [-1,1] \times [-1,1] \times [-1,1],\ \zeta_{g3} \in [0,0.8]$ and widths selected as $\sigma_{gf1} = 3, \sigma_{g1} = 2, \sigma_{gf3} =$

$6, \sigma_{g3} = 6$. The neural network update law parameters are set as $\{\eta_1, \eta_2, \eta_3, \eta_4 = 0.001\}$ and $\{\Gamma_{gf1}, \Gamma_{g1}, \Gamma_{gf3}, \Gamma_{g3} = diag\{50.0\}\}$. As the value of velocity is very large, normalization (by maximum velocity value) of this variable is carried out. Also for generating the flight path angle demand, a value of $k_{hf} = 0.15$ was set in (24).

Figure 2. shows the response to a 2000 ft step altitude command for the nominal model. It is observed that the altitude converges to the desired value in a short time through tracking of the flight path angle. A smooth elevator deflection is observed to realize the altitude demand of the air vehicle, during which the throttle command is being initiated by the PI controller to maintain air speed at 15,060 ft/s. Figure 3. shows the response to a 100 ft/s step velocity command for the nominal model. Similarly, the airspeed converges to a desired value in a short time with a smooth throttle command generated by the PI controller and a suitable elevator deflection command generated by DSC based robust neural networks adaptive controller to keep the altitude at 110,000ft. Any change in speed demand is reflected in the altitude channel as a cross coupling and vice versa. This cross coupling effect is also seen to have been effectively managed. Simulations are also conducted with parametric uncertainties in which the parameters, $\Delta m, \Delta I_{yy}$ and ΔCM_{α} are assigned double their maximum negative values and all other parameters are set to double their maximum positive values [2]. It can be observed from Figure 4. and Figure 5. that the designed DSC based robust adaptive neural networks controller is able to keep the system stable with reasonable control effort, and thus demonstrates robustness to parameter uncertainties. Again altitude and speed demands are met with good tracking performance, indicating viability of the selected design procedure under considerable parameter uncertainty.

b. DSC with Sliding mode observer

Simulation of the closed loop system with sliding mode observer is also carried out to ascertain the overall performance. The controller parameters used are the same as used in the case without the sliding mode observer, while the sliding mode observer parameters as given in section V are used. The nonlinear functions $\hat{f}_{qc}(\hat{\gamma}, \hat{\theta}_p, q, \delta_E, V)$ and $\hat{f}_{\gamma c}(\hat{\gamma}, \hat{\theta}_p, V)$ are approximated with centers evenly spaced in $\zeta_{qc} \in [-0.2,0.2] \times [-0.2,0.2] \times [-0.2,0.2] \times [-0.2,0.2] \times [-0.2,0.2]$, $\zeta_{\gamma c} \in [0,2] \times [0,2] \times [0,2]$ and widths selected as $\sigma_{qc} = 2, \sigma_{\gamma c} = 2$. The neural network update law parameters are set as $\eta_5 = 0.001, \eta_6 = 1 \times 10^{-5}, \Gamma_{qc} = diag\{300\}$, and $\Gamma_{\gamma c} = diag\{9000\}$.

Figure 6. shows the response to a 2000 ft step altitude command with parametric uncertainty and initial state error of 1.5 degree in α and other states set to their trim conditions. It can be observed that the altitude demand is being satisfied with a reasonable control effort, and also a good following of the required air speed demand is met. A slight degradation in tracking performance is observed, which is natural as now the observer is being used instead of a direct measurement of the flight path angle and angle of attack through costly sensors.

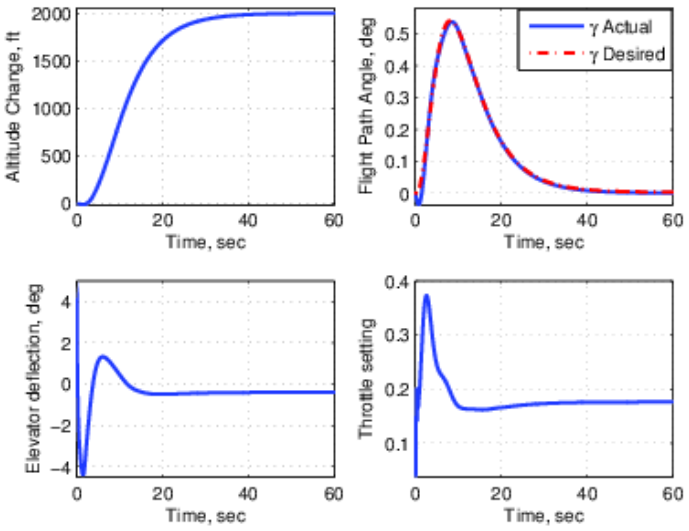

Figure 2. Response to a 2000-ft step-altitude command for the nominal model.

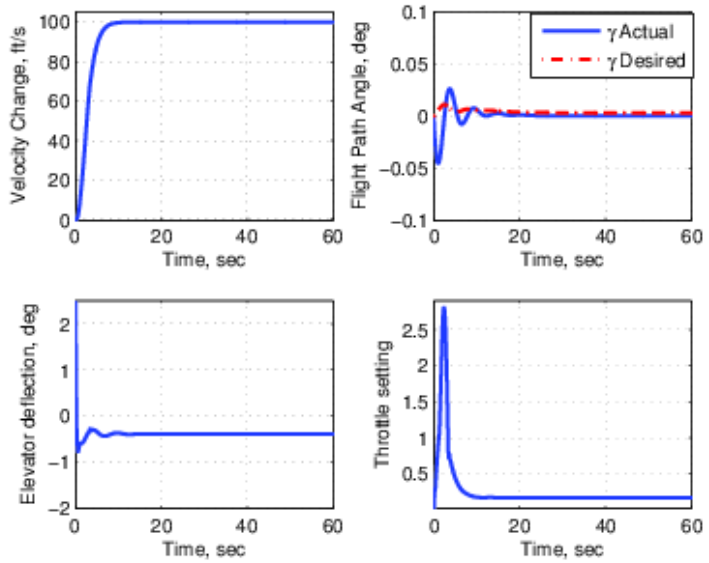

Figure 3. Response to a 100-ft/s step-velocity command for the nominal model.

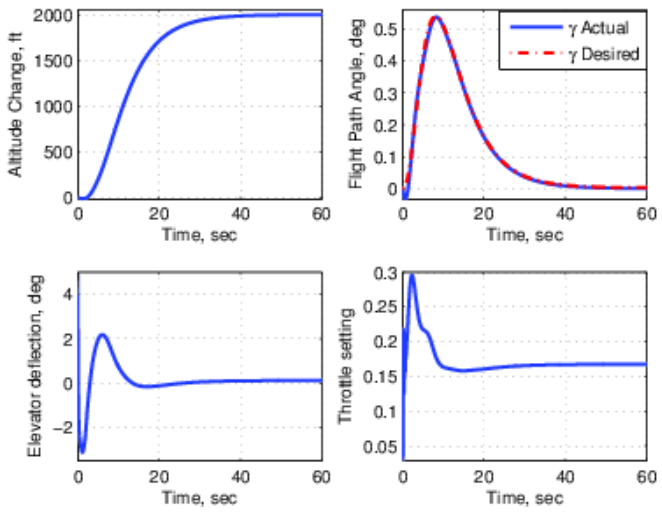

Figure 4. Response to a 2000-ft step-altitude command with parameter uncertainties.

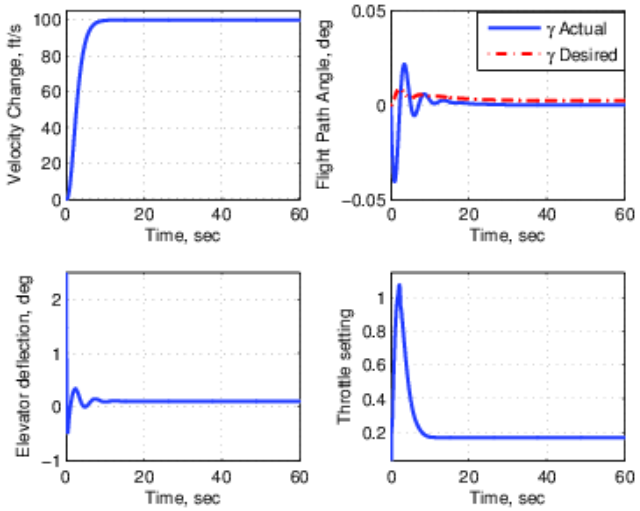

Figure 5. Response to a 100-ft/s step-velocity command with parameter uncertainties.

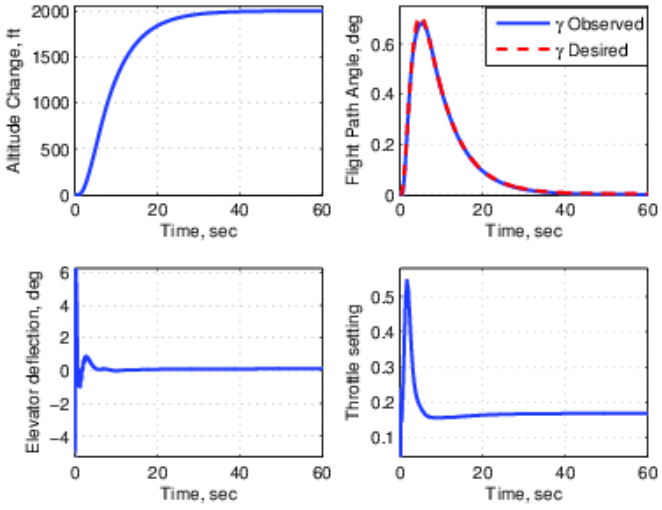

Figure 6. Response to a 2000-ft step-altitude command with parameter uncertainties and $\alpha(0) =$ 1.5 degree with sliding mode observer.

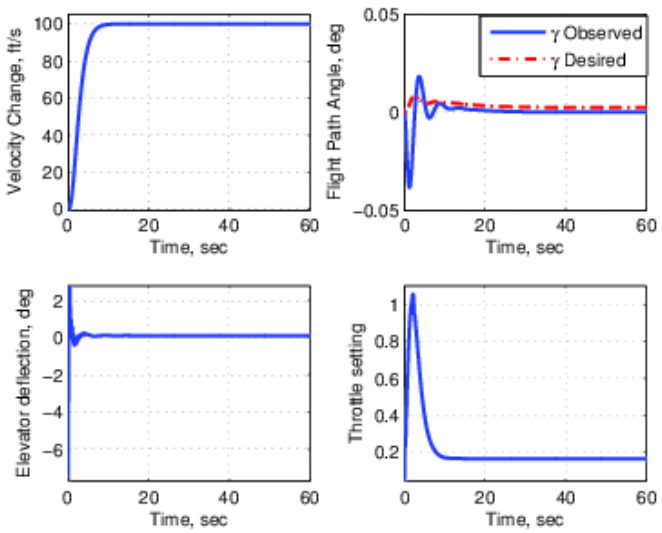

Figure 7. Response to a 100-ft/s step-velocity command with parameter uncertainties and $\alpha(0) = 1.5$ degree with sliding mode observer.

Figure 7. shows the response to a 100 ft/s step velocity command with parametric uncertainty and initial state error of 1.5 degree in α and other states set to their trim conditions.The air speed controller is able to maintain the desired air speed and the altitude controller keeps a strict control on the altitude tracking. The effect of cross channel coupling can be seen to be managed satisfactorily, revealing plausability of the design scheme. The overall closed loop system with the sliding mode observer is able to give reasonable performance even under parametric uncertainty.

VIII. CONCLUSIONS

The design procedure in this work employs a proportional integral controller and a dynamic surface controller for tracking the air speed and altitude demands respectively. The radial basis function neural networks by virtue of their approximation property are able to capture the uncertain nonlinear functions, that enables the dynamic surface control law to be robust to parametric uncertainties. Unlike the traditional backstepping scheme, the consequent control law structure of the dynamic surface control scheme is simpler and thus more suitable for practical implementation. By a suitable selection of design parameters, uniform ultimate stability of all the signals of the closed loop system is ensured. In a practical system, measurement of flight path angle and angle of attack requires costly sensors, thus a sliding mode observer is designed (with neural networks to approximate the smooth nonlinear functions), to observe these angles.

Nonlinear simulation of a flight vehicle with and without the observer reveals that the proposed controller design scheme is robust to parametric uncertainties and is able to give satisfactory performance even for a large change in parametric uncertainties.

REFERENCES

[1] H. Xu , M. Mirmirani, and P. Ioannou, “Adaptive Sliding Mode Control Design for A Hypersonic Flight Vehicle,” Journal of Guidance, Control and Dynamics, Vol. 27, No. 5, 2004, pp. 829-838. doi: 10.2514/1.12596

[2] O. Rehman, B. Fidan, and I. R. Petersen, “Robust Minimax Optimal Control of Nonlinear Uncertain Systems Using Feedback Linearization with Application to Hypersonic Flight Vehicles,” Proceedings of 48th IEEE Conference on Decision and Control, Shanghai, China, 2009, pp. 720-726. doi: 10.1109/CDC.2009.5399983

[3] Q. Wang, and R. Stengel, “Robust Nonlinear Control of a Hypersonic Aircraft,” Journal of Guidance, Control and Dynamics, Vol. 23, No. 4, 2000, pp. 577-585. doi: 10.2514/2.4580

[4] L. Fiorentini, A. Serrani, M. Bolender, and D. Doman, “Nonlinear Control of a Hypersonic Vehicle with Structural Flexibility,” Proceedings of 47th IEEE Conference on Decision and Control, Cancun, Mexico, 2008, pp. 578-583. doi: 10.1109/CDC.2008.4739001

[5] T. Lee, and Y. Kim, “Nonlinear Adaptive Flight Control Using Backstepping and Neural Networks Controller,” Journal of Guidance, Control and Dynamics, Vol. 24, No. 4, 2001, pp. 675-682. doi: 10.2514/2.4794

[6] M. Krstic, P. Kokotovic, and I. Kanellakopoulos, Nonlinear and Adaptive Control Design, Wiley, New York, NY, 1995, Chap. 3.

[7] I. Kanellakopoulos, P. Kokotovic, and A. S. Morse, “Systematic Design of Adaptive Controllers for Feedback Linearizable Systems,” IEEE Transactions on Automatic Control, Vol. 36, No. 11, 1991, pp. 1241-1253. doi: 10.1109/9.100933

[8] D. Swaroop, J. K. Hedrick, P. P. Yip, and J. C. Gerdes, “Dynamic Surface Control for a Class of Nonlinear Systems.” IEEE Transactions on Automatic Control, Vol. 45, No. 10, 2000, pp. 1893-1899. doi:10.1109/TAC.2000.880994

[9] B. Song, A. Howell, and K. Hedrick, “Dynamic Surface Control Design for a Class of Nonlinear Systems,” Proceedings of 40th IEEE Conference on Decision and Control, Orlando, Florida, 2001, pp. 2797-2802. doi: 10.1109/2001.980697

[10] L. Fiorentini, and A. Serrani, “Nonlinear Adaptive Control Design for Non-minimum Phase Hypersonic Vehicle Models with Minimal Control Authority,” Proceedings of 48th IEEE Conference on Decision and Control, Shanghai, China, 2009, pp. 1405-1410. doi:10.1109/CDC.2009.5400744

[11] M. Kuipers, P. Ioannou, and M. Mirmirani, “Analysis of an Adaptive Mixing Control Scheme for an Airbreathing Hypersonic Vehicle Model,” Proceedings of 48th IEEE Conference on Decision and Control, Shanghai, China, 2009, pp. 3148-3153. doi: 10.1109/ACC.2009.5160574

[12] L. Fiorentini, A. Serrani, M. Bolender, and D. Doman, “Nonlinear Robust Adaptive Control of Flexible Air-Breathing Hypersonic Vehicles, ” Journal of Guidance, Control and Dynamics, Vol. 32, No. 2, 2009, pp. 401-416. doi: 10.2514/1.39210.

[13] L. Fiorentini, A. Serrani, M. Bolender, and D. Doman, “Nonlinear Robust/Adaptive Controller Design for an Air-Breathing Hypersonic Vehicle Model,” AIAA Guidance, Navigation, and Control Conference and Exhibit, AIAA Paper 2007-6329, 2007.

[14] B. Fidan, M. Kuipers, M. Mirmirani, and P. Ioannou, “Longitudinal Motion Control of Air-Breathing Hypersonic Vehicles Based on Time-Varying Models,” 14th AIAA International Space Planes and Hypersonic Systems and Technologies Conference, AIAA Paper 2006-8074, 2006.

[15] D.X. Gao, Z.Q. Sun, and T. R. Du, “Dynamic Surface Control for Hypersonic Aircraft Using Fuzzy Logic System,” Proceedings of IEEE International Conference on Automation and Logistics, Jinan, China, 2007, pp. 2314-2319. doi: 10.1109/ICAL.2007.4338963

[16] J. Park, and I. W. Sandberg, “Universal Approximation Using Radial-Basis Function Networks,” Neural Computation., Vol. 3, No. 2, 1991, pp. 246-257. doi: 10.1162/neco.1991.3.2.246

[17] J.J.E. Slotine, J.K. Hedrick, and E. A. Misawa, “On Sliding Observers for Nonlinear Systems”, Journal of Dynamic Systems, Measurement and Control, Vol. 109, No. 3, 1987, pp. 245-252.

[18] J.J.E. Slotine, and W. Li, Applied Nonlinear Control, Prentice Hall, New Jersey, 1991, Chap. 7.

[19] W. Perruquetti, and J.P. Barbot, Sliding Mode Control in Engineering, Marcel Dekker, Inc., New York, 2002, Chap. 4.